Magnetic field effects on neutron diffraction in the antiferromagnetic phase of UPt_3

Juana Moreno and J. A. Sauls
Department of Physics and Astronomy, Northwestern University, Evanston, Illinois 60208
(Received 3 April 2000; revised manuscript received 12 September 2000; published 19 December 2000)

We discuss possible magnetic structures in UPt_3 based on our analysis of elastic neutron-scattering experiments in high magnetic fields at temperatures $T<T_N$. The existing experimental data are compatible with a true antiferromagnetic order displaying a single-**q** antiferromagnetic structure with three independent domains. For modest in-plane spin-orbit interactions, the Zeeman coupling between the antiferromagnetic order parameter and the magnetic field induces a rotation of the magnetic moments, but not an adjustment of the propagation vector of the magnetic order. A triple-**q** magnetic structure is also consistent with neutron experiments, but in general leads to a nonuniform magnetization in the crystal. New experiments involving higher fields and polarized neutrons could decide between these structures.

DOI: 10.1103/PhysRevB.63.024419 PACS number(s): 75.25.+z, 74.70.Tx, 75.20.Hr

I. INTRODUCTION

The coexistence of antiferromagnetic and superconducting order for five of the six heavy fermion superconductors suggests a deep connection between these two aspects of heavy fermion physics. In these materials the *f* electrons are involved in the superconducting transition, just as they are in the formation of the coherent heavy fermion band, but their precise role in the development of the unconventional superconducting phase is still unclear.

The magnetic field versus temperature phase diagram of UPt_3 provided compelling evidence of unconventional superconductivity in U-based heavy fermion materials.[1–3] In order to explain the phase diagram of UPt_3 several authors proposed a multicomponent order parameter based on a multidimensional representation of the hexagonal point group.[4–8] In these models a weak symmetry breaking field (SBF) is invoked. This SBF lifts the degeneracy of the multidimensional representation and leads to multiple transitions at lower temperatures and higher fields (see also the reviews in Refs. 7 and 9).

A natural candidate for the role of SBF is the weak antiferromagnetic order shown by neutron scattering measurements below $T_N=6$ K.[10–12] The ordered moment is unusually small, only $0.02\mu_B$ per U atom, and is directed in the basal plane, thus breaking the in-plane hexagonal symmetry. Evidence in support of an antiferromagnetic SBF coupled to the superconducting order parameter is based on the correlation between changes in the magnitude of the ordered moment and the splitting of the double transition. Both the splitting and the AFM order parameter are suppressed under applied pressure of $p_c\approx 3.5$ kbar.[13,14] The effect of Pd is the opposite; the splitting and the ordered moment increase with increasing Pd substitution.[15]

However, the character of the antiferromagnetic order is still unclear. Most thermodynamic and transport measurements have failed to detect a signature of AFM ordering near $T_N\simeq 6$ K.[16–19] However, evidence of magnetic ordering is observed to onset at T_N in the magnetoresistance.[20] The transition has other unusual characteristics as well, including finite range correlations, $\xi_{\rm AFM}\sim 300-500$ Å, depending on the crystalline direction and sample. By contrast, $(U,Th)(Pd,Pt)_3$ alloys exhibit AFM ordering at $T_N\approx 6$ K, but with ordered moments of conventional size, $\mu\sim 0.65\mu_B$/U ion, and resolution-limited Bragg peaks at the same positions as pure UPt_3.[21,22] Based on these facts, several authors have argued that the anomaly at 6 K does not indicate the onset of true long range magnetic ordering but finite-range AFM correlations,[23] which may also be fluctuating on time scales of order 5×10^{-10} s to 10^{-7} s.[24]

Given the uncertainties about the nature of the magnetic state in UPt_3, studies of the field dependence of the magnetic order were performed with the purpose of clarifying these issues. Two experimental groups have measured neutron scattering ratios in magnetic fields up to 3.5 (Ref. 25) and 12 T.[26] Both studies deduced that applied magnetic fields have no effect on the magnetic order of UPt_3, whether it be in aligning the moments or in domain selection. These previous conclusions support the view of fluctuating magnetic moments. However, our analysis and interpretation of these experiments leads to the conclusion that there is still room for a conventional dependency on the magnetic field and that additional neutron scattering data is necessary to clarify this issue.

Our analysis is based on the conventional theory of neutron scattering in magnetically ordered crystals and is summarized in Sec. II in the context of UPt_3. In Sec. III we present our analysis of the two sets of data that have been reported on the field dependence of the neutron scattering intensities. We also present the model-independent theoretical results for the ratio of the zero- and high-field limits for the measured neutron scattering intensities. Although this ratio does not depend on theoretical details, a complete description of the field evolution of the neutron scattering intensity requires a detailed analysis of the competing magnetic energies, as well as models for the possible domain structures that may be present in UPt_3. Thus, a free energy functional for AFM structures in UPt_3 is discussed in Sec. IV; the key features that enter our analysis are in-plane anisotropy energy, the Zeeman coupling to the AFM order parameter and the stiffness energy originating from the gradient energy and the domain-wall structure. The Dzyaloshinskii-Moriya coupling is also included in the free

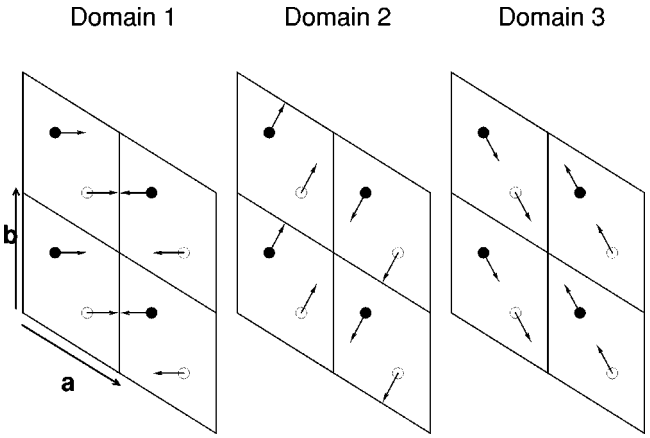

FIG. 1. The three equivalent domains for the configuration with propagation vector $\vec{q}_1=\vec{a}_1^*/2$. The other two configurations $[\vec{q}_2=\vec{a}_2^*/2,\vec{q}_3=(\vec{a}_1^*-\vec{a}_2^*)/2]$ also present identical domain structures. Black filled circles represent U atoms in the $z=c/4$ plane, empty circles represent U atoms on the $z=3c/4$ plane.

energy. This term generates a small induced ferromagnetic moment driven by the AFM order parameter, and leads to a correction to the scattering intensities close to the Neèl transition. In Sec. V we discuss the implications of a triple-**q** structure in UPt_3, and we point out that the existing neutron scattering data does not rule out such a structure. Section VI summarizes the main conclusions of the paper and suggests additional experiments that should resolve some of the open questions about the magnetic structure of UPt_3.

II. NEUTRON DIFFRACTION AND ANTIFERROMAGNETIC ORDER

We start from the conventional assumption of tiny antiferromagnetically ordered moments at each U site. These moments ($\vec{m}$) are assumed to lie on the basal plane due to a strong uniaxial anisotropy arising from spin-orbit coupling. In addition, there is an in-plane (hexagonal) anisotropy energy which favors alignment of the moments along any of the three directions perpendicular to the hexagonal lattice vectors (Fig. 1).

Neutron-scattering and x-ray experiments[10–12] show antiferromagnetic order with three possible propagation vectors $\vec{q}_1=\vec{a}_1^*/2,\vec{q}_2=\vec{a}_2^*/2,\vec{q}_3=(\vec{a}_1^*-\vec{a}_2^*)/2$, where $\vec{a}_1^*=(4\pi/\sqrt{3}a)(1,0,0)$, $\vec{a}_2^*=(4\pi/\sqrt{3}a)(1/2,\sqrt{3}/2,0)$, and $\vec{a}_3^*=(2\pi/c)(0,0,1)$ are the reciprocal vectors of the hexagonal lattice with dimensions $a=5.74$ Å and $c=4.89$ Å. The two U moments in each crystallographic unit cell have to align ferromagnetically in order to account for most of the zero-intensity Bragg points in the diffraction pattern. But, in general, the magnetic structure cannot be fully determined by standard neutron-diffraction experiments, since these experiments provide information only about the Fourier components of the magnetic moment. Single- and multi-**q** magnetic structures display the same magnetic Bragg peaks, and cannot be distinguished unless uniaxial stress or a magnetic field is applied.[27]

The magnetic neutron scattering rate per solid angle is proportional to[27,28]

$$\left(\frac{d\sigma}{d\Omega}\right)_{\vec{Q}} \propto \sum_{\vec{Q}_m} |F_{M\perp}(\vec{Q})|^2 \delta(\vec{Q}-\vec{Q}_m), \tag{1}$$

where $\vec{Q}$ is the momentum transfer, $\vec{Q}_m$ are the momenta of the magnetic Bragg peaks, and $F_{M\perp}(\vec{Q})$ is the component of the magnetic structure factor perpendicular to the momentum transfer. We can define the magnetic structure factor as

$$\vec{F}_M(\vec{Q})=\frac{1}{N}\sum_{n,j} \vec{m}_{nj} f_{nj}(\vec{Q}) e^{i\vec{Q}\cdot\vec{R}_{nj}-W_j}, \tag{2}$$

where $\vec{m}_{nj}$ is the magnetic moment of the jth ion in the nth unit cell, f_{nj} is its atomic form factor, $\vec{R}_{nj}$ is its position, and W_j is the Debye-Waller factor.

The spatial distribution of magnetic moments can be Fourier expanded as $\vec{m}_{n,j}=\Sigma_{\vec{q}}\vec{m}_{\vec{q},j}e^{-i\vec{q}\cdot\vec{R}_n}$, where the form factor associated with this multi-**q** magnetic structure is $\vec{F}_M(\vec{Q}=\vec{Q}_{nm}+\vec{q})=\Sigma_j\vec{m}_{\vec{q},j}f_j(\vec{Q})e^{i\vec{Q}\cdot\vec{r}_j-W_j}$ where $\vec{r}_j$ are the positions of the magnetic ions in the unit cell and $\vec{Q}_{nm}$ label the reciprocal lattice vectors. Thus, in a material with only one type of magnetic ion the scattering rate becomes

$$\left(\frac{d\sigma}{d\Omega}\right)_{\vec{Q}} \propto \sum_{\vec{Q}_{nm},\vec{q}} [1-(\hat{Q}\cdot\hat{m}_{\vec{q}})^2]|f(\vec{Q})|^2 \left|\sum_{\vec{r}_i} e^{i\vec{Q}\cdot\vec{r}_i}\vec{m}_{\vec{q}}\right|^2 \times \delta[\vec{Q}-(\vec{Q}_{nm}+\vec{q})]. \tag{3}$$

Thus, the UPt_3 diffraction pattern can either be associated with a triple-**q** structure where $\vec{q}_1$, $\vec{q}_2$, and $\vec{q}_3$ are present at each uranium site or with a single-**q** structure where separate regions of the crystal will order with different propagation vectors. It has been inferred from the fact that there is no intensity at the $\vec{q}_1=[1/2,0,0]$ position that the magnetic moment lies parallel to its propagation vector.[21,22] This is the case in the U monochalcogenides and U monopnictides with cubic NaCl structure, which order with magnetic moments $\mu\simeq 1-3\mu_B$.[27] A moment directed along $\vec{q}$ would also occur for a triple-**q** structure, but it is not clear that this condition must be fulfilled in the single-**q** structure. The intensity of $\vec{q}_2=[0,1/2,0]$ and $\vec{q}_3=[1/2,-1/2,0]$ peaks has not been reported for UPt_3. It is possible that the sample preparation methods make domain ''1'' (Fig. 1) preferable over domains ''2'' and ''3.'' However, measuring the intensity of these three peaks in the same single crystal would allow one to determine if the magnetic moments do lie parallel to the propagation vector of the domain.

III. FIELD DEPENDENCE OF THE NEUTRON SCATTERING INTENSITIES

Now we discuss the field dependence of the magnetic neutron scattering intensity for single-**q** structures. In a later section we comment on the possibility of a triple-**q** magnetic structure. The magnetic unit cell of a single-**q** structure re-

sults from doubling the hexagonal unit cell along one in-plane direction, reducing the hexagonal symmetry to orthorhombic.

Transmission electron microscope images provide direct observation of basal plane, as well as prism plane, stacking faults in pure single crystals.[29] These defects are observed even in the crystals with the highest residual resistance ratios. We hypothesize that these defects pin AFM domain walls in the ab plane and fix the spatial distribution of domains.[30,31]

In an antiferromagnet the Zeeman energy prefers the staggered magnetization to be perpendicular to the field. Thus, a sufficiently strong magnetic field applied in the hexagonal plane will give rise to domain reorientation by overcoming the in-plane anisotropy energy. The magnitude of the staggered magnetization will remain roughly the same, modulated only by a small in-plane anisotropy energy.[32] Therefore, for a given magnetic Bragg peak, the ratio between the scattering rate at high field and at zero field is[33]

$$r=\frac{d\sigma/d\Omega|_{H\to\infty}}{d\sigma/d\Omega|_{H=0}}\approx\frac{\langle 1-(\hat{Q}\cdot\hat{m}_{H\to\infty})^2\rangle}{\langle 1-(\hat{Q}\cdot\hat{m}_{H=0})^2\rangle}, \tag{4}$$

where $\langle\cdots\rangle$ refers to an average over domains.

Let us analyze the experimental data based on Eq. (4). The staggered magnetization lies on the basal plane, $\hat{m}=(\cos\theta,\sin\theta)$. Van Dijk *et al.*[26] chose a configuration with H parallel to the a axis [$\theta_H=-30°$ in Eq. (9)] and a momentum transfer $\vec{Q}=[1/2,0,1]=2\pi[(1/\sqrt{3}a),0,(1/c)]$, which gives $\hat{Q}=(0.441,0,0.897)$ and

$$r=\frac{1-[0.441\cos(\theta_H+\pi/2)]^2}{\langle 1-[0.441\cos(\theta)]^2\rangle}=1.05 \tag{5}$$

for three equally populated magnetic domains. This ratio can be increased to $r=1.18$ by assuming that only the domain with the staggered magnetization parallel to the propagation vector is populated (domain ''1'' in Fig. 1). Thus, even in the case of complete domain reorientation, the neutron scattering rate at $\vec{Q}=[1/2,0,1]$ in high fields can increase at most by 18% over its value at zero field. Figure 2 shows the experimental data and the theoretical curves for a model with equally populated domains and for a model with only domain ''1'' populated. Although the theoretical calculation associated with domain ''1'' is in good agreement with the data, it is not possible to conclude whether or not the U moments rotate with the field because of the small change in intensity that is expected for this Bragg peak and the large error bars that are reported for the intensity. Note that the error bars for this measurement are comparable to the maximum change in the intensity ratio. In our calculation we have assumed an anisotropy field of $H_{an}=1.5$ T. However, much smaller values are consistent with the limited data. The precise value of the additional parameters in our model play a role only in the region of small magnetic fields. For fields $H>2H_{an}$ the ratio between the intensity at high fields and at zero field saturates at its upper limit, which is determined by purely geometrical arguments.

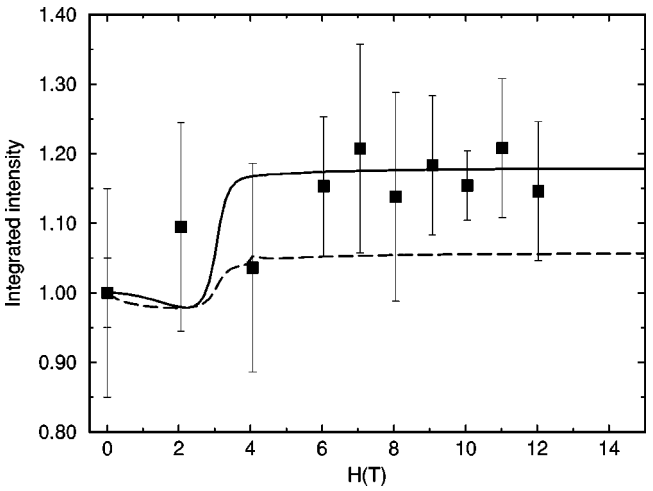

FIG. 2. Relative integrated intensity of the magnetic Bragg peak $\vec{Q}=[1/2,0,1]$ as a function of applied magnetic field. H is parallel to the a axis. The solid line corresponds to a crystal with only domain 1 populated, and the dashed line represents a sample with three equally populated domains. The parameters we used [refer to Eq. (9)] are $H_{an}=1.5$ T, $U_{an}=0.02U_{ex}$, and $r_{st}=0.02$. The calculated curves are compared with measurements of van Dijk *et al.* (Ref. 26) (black squares).

Earlier analysis[26] was based on the assumption that the staggered magnetic moment is *always* parallel to its propagation vector. Thus, it was expected that a sufficiently high magnetic field parallel to the a axis would select domain 2 with propagation vector $\vec{q}_2$ throughout the sample. As a consequence, the magnetic intensity at $\vec{Q}=[1/2,0,1]=\vec{q}_1+[0,0,1]$ was expected to drop to zero. However, as we show in Fig. 2, if we assume that the spatial distribution of domain walls is pinned, the form factors for $\vec{Q}=[1/2,0,1]$, which is a vector mostly out of the hexagonal plane, lead to a much smaller variation of the intensity with the field.

Larger expected ratios between the low- and high-field intensities are obtained with the experimental setup used by Lussier *et al.*[25] They measured the neutron scattering cross section at three different momentum transfers, all in the basal plane: $\vec{Q}_1=[1/2,1,0]$, $\vec{Q}_2=[-3/2,1/2,0]$, and $\vec{Q}_3=[-1,3/2,0]$. The magnetic field was oriented along the **b** axis. Lussier *et al.*[25] report data for $\vec{Q}_1$ and $\vec{Q}_2$, and magnetic fields up to $3.5T$. We can estimate from Eq. (4) the ratio between high- and zero-field intensity for any distribution of domains in the crystal. A crystal with equally populated domains will display the following ratios for the neutron scattering rate at high fields and zero field:

$$r(\vec{Q}_1)=0.86,\quad r(\vec{Q}_2)=0.21,\quad r(\vec{Q}_3)=1.93. \tag{6}$$

If domain 3 is unpopulated and domains 1 and 2 are equally populated the ratios should be

$$r(\vec{Q}_1)=1.60,\quad r(\vec{Q}_2)=0.20,\quad r(\vec{Q}_3)=1.38, \tag{7}$$

and if only the domain with the magnetization parallel to the propagation vector is occupied (e.g., domain 1 for $\vec{Q}_1$) then

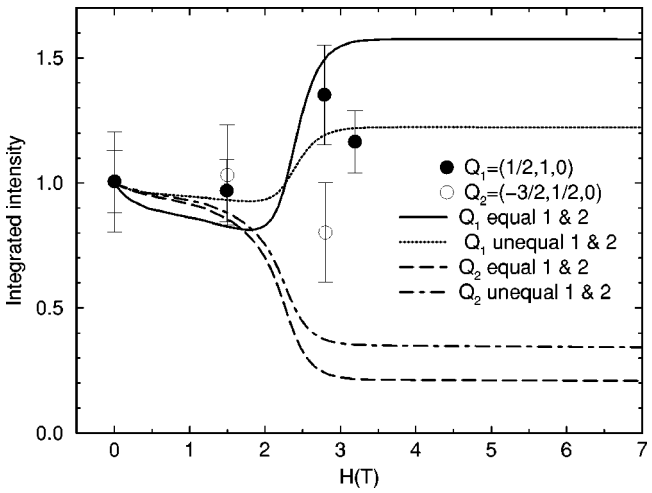

FIG. 3. Normalized integrated scattering intensity as a function of the field for $\vec{Q}_1=[1/2,1,0]$ and $\vec{Q}_2=[-3/2,1/2,0]$. The magnetic field points along the b axis. Calculated curves are compared with measurements of Lussier *et al.* (Ref. 25). We show calculations for two domain structures: domain 1 and 2 equally populated and domain 1 on 3/4 of the sample, domain 2 on 1/4. We used the same parameters as those for Fig. 2: $H_{\rm an}=1.5$ T, $U_{\rm an}=0.02U_{\rm ex}$, and $r_{\rm st}=0.02$.

$$r(\vec{Q}_1)=1, \quad r(\vec{Q}_2)=0.25, \quad r(\vec{Q}_3)=2.25. \tag{8}$$

Figure 3 displays the experimental data of Ref. 25, and theoretical calculations for two samples, one with domains 1 and 2 equally populated at zero field, another with domains 1 and 2 unequally populated. The parameters of the model are the same ones used to fit the data at $\vec{Q}=[1/2,0,1]$ in Fig. 2. We conclude that the limited data for $\vec{Q}_1$ and $\vec{Q}_2$ is roughly consistent with either one or two unequally populated domains, particularly if $H_{\rm an}\gtrsim 2.5$ T. Previous analysis of these results was also based on the assumption that the propagation vector of the magnetic domains follows the rotation of the magnetic moments.[25] Thus, at high fields it was expected that the intensity of the $\vec{Q}_2$ and $\vec{Q}_3$ peaks would be suppressed to zero, while increasing the intensity of the $\vec{Q}_1$ peak to roughly three times its zero field value.

IV. FREE ENERGY FUNCTIONAL

The theoretical curves displayed in the figures have been calculated using the free energy functional[34,32]

$$\begin{aligned}\overline{F}_{\rm AFM}=&-2(1-\overline{T})|\vec{m}_0|^2+|\vec{m}_0|^4+\overline{U}_{\rm an}|\vec{m}_0|^6[r_6-\cos(6\theta)]\\&+\overline{U}_{\rm an}\overline{H}^2|\vec{m}_0|^2\cos^2(\theta-\theta_H)\\&+r_D\overline{U}_{\rm an}\overline{H}|\vec{m}_0||\sin(\theta-\theta_H)|\\&+r_{st}|\vec{m}_0|^2\left[\left(\frac{\partial[\cos(\theta)]}{\partial H}\right)^2+\left(\frac{\partial[\sin(\theta)]}{\partial H}\right)^2\right],\end{aligned} \tag{9}$$

where all energies are measured in units of the exchange energy $U_{\rm ex}$, which is defined as the absolute value of the free energy at zero temperature and field in the absence of any anisotropy energy. The magnetic order parameter is restricted to the basal plane by the large uniaxial anisotropy energy [not shown in Eq. (9)] and it is measured with respect to the antiferromagnetic order parameter in the exchange approximation $\vec{m}_0=\vec{m}/|\vec{m}_{\rm ex}|=|\vec{m}_0|(\cos\theta,\sin\theta,0)$. The renormalized temperature is defined as $\overline{T}=T/T_N$, with T_N as the Néel temperature. The magnetic field $\overline{H}$ is measured in units of the in-plane anisotropy field $H_{\rm an}$. The first two terms of the free energy correspond to the exchange energy. For $\overline{T}<1$ antiferromagnetic order with magnetic moment $|\vec{m}_0|=|\vec{m}|/|\vec{m}_{\rm ex}|=\sqrt{1-\overline{T}}$ and free energy $\overline{F}_{\rm AFM}=F_{\rm AFM}/U_{\rm ex}=-(1-\overline{T})^2$ is stable. The sixth-order term is the leading term in the in-plane anisotropy energy; it favors alignment along the three directions perpendicular to the hexagonal lattice vectors $\theta=n(\pi/3)$, where n is an integer. The in-plane anisotropy energy induces a hexagonal modulation of the upper critical field as a function of the orientation of the field in the basal plane.[35] From the magnitude of this hexagonal modulation we estimate an anisotropy energy of $\overline{U}_{\rm an}=U_{\rm an}/U_{\rm ex}\sim 0.02$.[32] The parameter r_6 must be bigger than one in order to have a stable free energy. We use $r_6=1.5$ in our calculations, however, its precise value does not play any significant role in the minimization of the free energy.

The fourth term is the Zeeman energy for an antiferromagnet $F_Z=g(\vec{m}\cdot\vec{H})^2$ which is quadratic in H and favors perpendicular alignment $(g>0)$ of the staggered moment and the magnetic field. This term can be written in the form

$$F_Z=\frac{U_{\rm an}}{U_{\rm ex}}\left(\frac{H}{H_{\rm an}}\right)^2\left(\frac{\vec{m}}{|\vec{m}_{\rm ex}|}\right)^2\cos^2(\theta-\theta_H), \tag{10}$$

where $H_{\rm an}=(1/|\vec{m}_{\rm ex}|)\sqrt{U_{\rm an}/(gU_{\rm ex})}$ and θ_H is the angle of the magnetic field with the $\vec{a}_1^*$ reciprocal vector.

The fifth term in Eq. (9) is the Dzyaloshinskii-Moriya term describing the *linear* coupling of the sublattice magnetization to the magnetic field $F_D=g'\mathbf{d}\cdot(\mathbf{H}\times\mathbf{m}_0)$. This term corresponds to the Zeeman coupling of a weak ferromagnetic (FM) moment in systems which are predominantly antiferromagnetic. Its origin is the anisotropic superexchange coupling between magnetic moments $\sim\vec{D}_{ij}\cdot\vec{S}_i\times\vec{S}_j$, where $\vec{D}_{ij}$ are the Moriya vectors for different bonds on the lattice, and which are related to each other by lattice symmetries.[36,37] In the case of UPt_3, $\vec{D}_{ij}=0$ when i and j are nearest-neighbor U sites, while $\vec{D}_{ij}=\pm|d|\hat{c}$, independent of the direction of the staggered magnetic moment, when i and j refer to next-nearest-neighbor U atoms.[38] This superexchange coupling generates the Dzyaloshinskii term in the free energy which can be expressed as $\overline{F}_D=r_D\overline{U}_{\rm an}\overline{H}|\vec{m}_0||\sin(\theta-\theta_H)|$ shown in Eq. (9).

Finally, the last term in Eq. (9) describes the ''stiffness'' of the order parameter with respect to rotations in the ab plane. This stiffness originates from the formation of domains in which the staggered moment points in the same

direction within each domain. An inhomogeneous domain structure gives rise to domain walls separating differently oriented domains. The energy associated with the domain wall is obtained from the gradient energy $\kappa_{ijkl}(\partial m_j/\partial x_i)(\partial m_l/\partial x_k)$, which must be included in the free energy functional. For an individual domain wall, the gradient energy can be written as an integral over the domain wall surface Ω[39]

$$F_{\text{wall}} \propto \int_{\Omega} d\Omega \int_{\sigma_1}^{\sigma_2} \left[\left(\frac{\partial \hat{\mathbf{m}}_x}{\partial \sigma} \right)^2 + \left(\frac{\partial \hat{\mathbf{m}}_y}{\partial \sigma} \right)^2 \right] d\sigma, \qquad (11)$$

where σ is the coordinate perpendicular at each point to the wall surface. The width of the wall is given by $\sigma_2 - \sigma_1$ and $\hat{\mathbf{m}}_\mathbf{x}$, $\hat{\mathbf{m}}_\mathbf{y}$ are the components of the unit vector $\hat{\mathbf{m}} = \mathbf{m}/|\mathbf{m}|$. This unit vector satisfies the boundary conditions $\hat{\mathbf{m}}(\sigma_2) = \hat{\mathbf{m}}_{\text{eq}}(H + \Delta H)$ and $\hat{\mathbf{m}}(\sigma_1) = \hat{\mathbf{m}}_{\text{eq}}(H)$, where $\hat{\mathbf{m}}_{\text{eq}}(H)$ is the equilibrium orientation of the staggered magnetic moment in the presence of a magnetic field $\vec{H}$. In quasiequilibrium the direction of the magnetic moment evolves smoothly through the domain wall between its values corresponding to different equilibrium field orientations $\hat{\mathbf{m}}_{\text{eq}}(H + \Delta H)$ and $\hat{\mathbf{m}}_{\text{eq}}(H)$. By scaling the width of the domain wall to ΔH we obtain the stiffness energy in the form of the last term in Eq. (9).

The stiffness energy is important in the region of intermediate fields, where the normalized neutron intensity increases from a value close to the one at zero field to its value at high fields. The initial drop of the neutron intensity as a function of the applied field (Figs. 2 and 3) is a combined effect of the anisotropy and stiffness energies. This drop is due to an initial reduction of the magnitude of the magnetic moment. Small fields do not induce rotation; instead the magnitude of the staggered moment is reduced. Higher fields are able to rotate the moments by overcoming the anisotropy and stiffness energies. Consequently, the Zeeman energy is reduced to zero and the rotated moment recovers its value at zero field.

For low temperatures the effect of the Dzyaloshinskii-Moriya term is to generate a tiny ferromagnetic moment at the price of a small reduction in the magnitude of the staggered moment. However, for temperatures close to T_N, the Dzyaloshinskii-Moriya energy is comparable to the exchange energy, and leads to a significant reduction in the magnitude of the AFM moment and, as a consequence, the intensity of the magnetic Bragg peaks. We can define a crossover temperature in terms of the parameters of the free energy [Eq. (9)], $\overline{T}_D = 1 - \sqrt[3]{r_D^2 U_{\text{an}}^2 \overline{H}^2}$. Although the staggered moment vanishes precisely at the Néel temperature, for $\overline{T}_D < \overline{T} < 1$ the moment decreases rapidly before the transition at $\overline{T} = 1$. Thus, $\overline{T}_D$ could be misidentified as the Néel temperature of the sample. The Dzyaloshinskii-Moriya term provides an explanation for the crossing of the intensity curves for zero and high fields as a function of temperature as shown in Fig. 4.

The Dzyaloshinskii-Moriya coupling also provides an explanation for the linear term in the field dependence of the magnetoresistance,[20] which onsets at the Neèl transition and increases for $T < T_N$. It has been shown that a linear term in the transverse magnetoresistance is present in antiferromagnetic structures admitting the existence of weak ferromagnetism.[40] Indeed it follows from Onsager relations for the resistivity that a magnetoresistance which is linear in field in a AFM requires the Dzyaloshinskii-Moriya coupling.

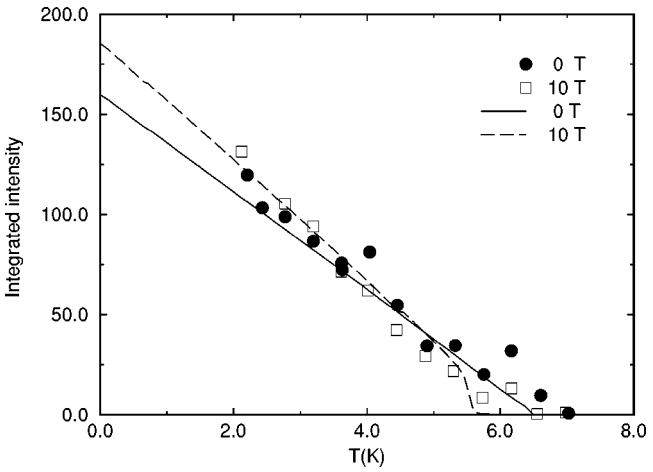

FIG. 4. Temperature dependence of the integrated intensity of the magnetic Bragg peak $\vec{Q} = [1/2,0,1]$ in a magnetic field of $H = 0$ and 10 T. The solid line represents a calculation at $H = 0$ T, and the dashed line shows the dependence at $H = 10$ T. The calculations assume that only domain 1 is populated, and we have used the same parameters as those used for the calculations shown in Fig. 2 plus a weak ferromagnetic coupling proportional to $r_D = 0.5$. The experimental data is that reported by van Dijk *et al.* (Ref. 26) at zero field (black circles) and at 10 T (white squares).

V. TRIPLE-q STRUCTURE

So far we have discussed single-**q** structures or multidomain single-**q** structures. Triple-**q** structures are also possible. By symmetry each of the Fourier components of the magnetization $\vec{m}_{\vec{q}_i}$ has the same amplitude. Triple-**q** antiferromagnetic order occurs in the NaCl-type monopnictide USb,[27] in the CsCl-type DyAg (Ref. 41) and NdZn,[42,43] and in the $AuCu_3$-type $TmGa_3$.[44] These materials are cubic and the three Fourier components $\vec{m}_{\vec{q}_i}$ point along mutually perpendicular axes leading to the condition of a uniform magnitude of the moment.[45]

For a triple-**q** structure in UPt_3, in order to explain the vanishing intensity at the (1/2,0,0) Bragg point we are required to have $\vec{m}_{\vec{q}_1}$ parallel to $\vec{q}_1$ and by symmetry the other two moments must also be parallel to their propagation vectors. Thus, the magnetic moment of both U ions in the nth unit cell is given by

$$\vec{m}_n = |m| \sum_{i=1}^{3} \hat{\mathbf{q}}_i e^{i(\phi_i - \vec{\mathbf{q}}_i \cdot \mathbf{R}_n)}. \qquad (12)$$

It can be easily shown that it is not possible to satisfy the condition of equal magnitude of the moment at every U site.

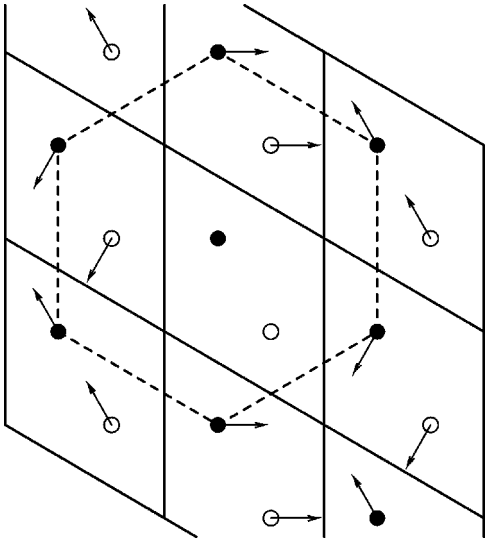

FIG. 5. Spatial distribution of the magnetic moments for a triple-**q** magnetic structure with equal values of the three phase factors, ϕ_i. Note that the two U ions in the center of the cell have zero net moment. Black filled circles represent U atoms in the $z=c/4$ plane, and empty circles represent U atoms in the $z=3(c/4)$ plane.

Most choices for the phases ϕ_1,ϕ_2,ϕ_3 produce a nonuniform distribution of the magnitude of the U magnetic moment.[46] For example, Fig. 5 displays a possible spatial distribution of the moments. The three Fourier components of the triple structure have been chosen with equal phase $\phi_1=\phi_2=\phi_3$. The magnetic unit cell is then constructed from four unit cells containing eight U ions, reducing the hexagonal symmetry to monoclinic. Note that the two U ions in the central cell have zero net moment, while the other six U ions have equal values for the magnitude of the moment.

Even though a triple-**q** magnetic structure in UPt_3 is compatible with the neutron-scattering experiments the resulting nonuniform magnetization is unusual, but not unique. The triple-**q** magnetic structure in UPt_3 is similar to the magnetically frustrated structure of the uranium intermetallic UNi_4B, which also has a hexagonal crystal lattice.[47] This material orders antiferromagnetically around $T_N=30$ K, with approximately 1/3 of the U spins remaining paramagnetic well below T_N. It has been suggested that the competition between the Kondo effect, the antiferromagnetic exchange interaction and the frustration of the crystallographic lattice is responsible for the unusual UNi_4B magnetic structure.[48] Such an interplay between competing interactions could also take place in UPt_3. However, to our knowledge, there is no other indication of such a frustrated magnetic structure in UPt_3.

Note that a triple-**q** structure does not preclude the coupling between the AFM and superconducting order parameters, which is considered a good candidate for the proposed SBF in the two-dimensional order parameter models for the superconducting phases.[4–9] The SBF coupling is nonvanishing for triple-**q** structures, except for the special case in which all three phases are identical. The coupling between the superconducting, $\vec{\eta}=(\eta_1,\eta_2)$, and the magnetic order parameters is $F_{\text{AFM-SC}}\propto A(|\eta_1|^2-|\eta_2|^2)+B(\eta_1\eta_2^*+\eta_1^*\eta_2)$, with $A=\Sigma_{n=1,4}[m_x^2(n)-m_y^2(n)]=4-2\cos^2(\phi_2-\phi_1)-2\cos^2(\phi_3-\phi_1)$, $B=2\Sigma_{n=1,4}[m_x(n)m_y(n)]=2\sqrt{3}[\cos^2(\phi_2-\phi_1)-\cos^2(\phi_3-\phi_1)]$, where the summation refers to the four unit cells contained in the magnetic unit cell shown in Fig. 5.

The hexagonal triple-**q** shown in Fig. 5 resembles the antiferroquadrupolar order reported for UPd_3.[49,50] Furthermore, Pt and Pd are isoelectronic, their nearest neighbor U-U distances are almost identical, and both systems have a hexagonal closed packed structures. However, the magnetic and electronic properties of UPt_3 and UPd_3 are very different. In fact UPd_3 is a localized material[51] with well-defined crystal-field levels.[52] Several measurements on UPd_3 show *two* phase transitions at 7 and 5 K.[53,54] The transition at 7 K is believed to correspond to a quadrupolar ordering of the U ions, which is accompanied by a modulated lattice distortion. The 5 K transition is magnetic, with an ordered moment that is very small, as in UPt_3, $\mu\simeq 0.01\mu_B$/U ion. But, the moments in UPd_3 are pointing out of the basal plane.[55]

VI. CONCLUSIONS

We have analyzed neutron diffraction data in the antiferromagnetic phase of UPt_3 at high magnetic fields.[25,26] The magnetic field dependence of the neutron scattering intensity is consistent with an antiferromagnetic order based on the most conventional assumption of a single-**q** structure with three equivalent domains. The field and temperature dependence of the neutron intensities[25,26] can be explained assuming reasonable parameters in a free energy functional. In our analysis, we also assume that defects, e.g., stacking faults which are observed even in the best single crystals,[29] pin the AFM domain walls.[30,31]

A triplet-**q** structure is also consistent with neutron scattering experiments. If realized the triple-**q** structure would imply a nonuniform, frustrated magnetic structure in the crystal. A similar frustrated structure is observed in UNi_4B. In this material the competition between the Kondo effect and the antiferromagnetic exchange interaction is fundamental to understand its magnetic structure.[48] This competition could also play a fundamental role in UPt_3.

We conclude with a brief discussion of possible neutron scattering experiments which might clarify the magnetic order in UPt_3. Systematic, zero-field measurements of the intensity of a number of magnetic peaks in the same single crystal will determine whether or not the magnetic moments are indeed parallel to the propagation vector. Using previous experimental arrangements[25] it would be very interesting to apply fields well above 3 T and measure the intensity at three independent momentum transfers. Although polarized inelastic neutron-scattering experiments have been performed in UPt_3,[56] the magnetic Bragg peaks have not been studied with polarized neutrons. Polarized elastic neutron-scattering would provide confirmation of the magnetic nature of the transition. This powerful method has been used successfully on UPd_3 to identify the magnetic nature of the second phase transition at $T_2=5$ K.[55]

ACKNOWLEDGMENTS

We thank Piers Coleman, Bill Halperin, and Robert Joynt for valuable discussions on this subject. The hospitality of the Aspen Center for Physics during the 1999 Summer workshop on unconventional order in metals is gratefully acknowledged. This research was supported by NSF Grants No. DMR 9705473, DMR 9972087, and DMR 91-20000 through the Science and Technology Center for Superconductivity.

[1] K. Hasselbach *et al.*, Phys. Rev. Lett. **63**, 93 (1989).
[2] A. Adenwalla *et al.*, Phys. Rev. Lett. **65**, 2298 (1990).
[3] G. Bruls *et al.*, Phys. Rev. Lett. **65**, 2294 (1990).
[4] D.W. Hess, T. Tokuyasu, and J.A. Sauls, J. Phys.: Condens. Matter **1**, 8135 (1989).
[5] K. Machida and M. Ozaki, J. Phys. Soc. Jpn. **58**, 2244 (1989).
[6] R. Joynt, J. Magn. Magn. Mater. **108**, 31 (1992).
[7] J.A. Sauls, Adv. Phys. **43**, 113 (1994).
[8] K. Machida and T. Ohmi, J. Phys. Soc. Jpn. **67**, 1122 (1998).
[9] R.H. Heffner and M.R. Norman, Comments Condens. Matter Phys. **17**, 361 (1996).
[10] G. Aeppli *et al.*, Phys. Rev. Lett. **60**, 615 (1988).
[11] E.D. Isaacs *et al.*, Phys. Rev. Lett. **75**, 1178 (1995).
[12] R.J. Keizer *et al.*, Phys. Rev. B **60**, 6668 (1999).
[13] T. Trappmann, H.v. Löhneysen, and L. Taillefer, Phys. Rev. B **43**, 13 714 (1991).
[14] S.M. Hayden *et al.*, Phys. Rev. B **46**, 8675 (1992).
[15] R.J. Keizer *et al.*, Phys. Rev. B **60**, 10 527 (1999).
[16] R.A. Fisher *et al.*, Solid State Commun. **80**, 263 (1991).
[17] H. Tou *et al.*, Phys. Rev. Lett. **77**, 1374 (1996).
[18] R.J. Keizer *et al.*, J. Phys.: Condens. Matter **11**, 8591 (1999).
[19] P. Dalmas de Réotier *et al.*, Phys. Lett. A **205**, 239 (1995).
[20] K. Behnia *et al.*, Physica B **165&166**, 431 (1990).
[21] A.I. Goldman *et al.*, Phys. Rev. B **34**, 6564 (1986).
[22] P. Frings *et al.*, J. Magn. Magn. Mater. **63&64**, 202 (1987).
[23] I.A. Fomin and J. Flouquet, Solid State Commun. **98**, 795 (1996).
[24] Y. Okuno and K. Miyake, J. Phys. Soc. Jpn. **67**, 3342 (1998).
[25] B. Lussier *et al.*, Phys. Rev. B **54**, R6873 (1996).
[26] N.H. van Dijk *et al.*, Phys. Rev. B **58**, 3186 (1998).
[27] J. Rossat-Mignod, G.H. Lander, and P. Burlet, in *Handbook on the Physics and Chemistry of Actinides*, edited by A.J. Freeman and G.H. Lander (Elsevier, Amsterdam, 1984), Vol. 1, p. 415.
[28] G.L. Squires, in *Introduction to the Theory of Thermal Neutron Scattering* (Cambridge University Press, Cambridge, 1978).
[29] J. Hong, Ph.D. thesis, Northwestern University, 1999.
[30] A. Amann *et al.*, Phys. Rev. B **57**, 3640 (1998).
[31] Pinning of the flux line lattice (for $\mathbf{H}||\mathbf{c}$) in the superconducting phases of very pure single crystals of UPt_3 was recently reported and attributed to stacking faults; A. Huxley *et al.*, Nature (London) **406**, 160 (2000); A. Huxley (unpublished).
[32] J.A. Sauls, Phys. Rev. B **53**, 8543 (1996).
[33] H. Kita *et al.*, J. Phys. Soc. Jpn. **63**, 726 (1994).
[34] A.F. Andreev and V.I. Marchenko, Usp. Fiz. Nauk. **132**, 3 (1980) [Sov. Phys. Usp. **23**, 1 (1980)].
[35] N. Keller *et al.*, Physica B **206&207**, 568 (1995).
[36] T. Moriya, Phys. Rev. **120**, 91 (1960).
[37] L. Shekhtman, O. Entin-Wohlman, and A. Aharony, Phys. Rev. Lett. **69**, 836 (1992).
[38] At each Uranium site three mirror planes, each of them including one of the nearest-neighbor U ions, intersect. Thus, $\vec{D}_{ij}$ for nearest-neighbor sites must be perpendicular to the mirror plane including i and j. As consequence, $\vec{D}_{ij}$ would lie in the basal plane, which contradicts the constraint $\vec{D}_{ij}||\mathbf{c}$ imposed by the hypothesis of magnetic moments confined to the basal plane. However, when i and j are next-near-neighbor U sites the only restriction is that $\vec{D}_{ij}$ must be invariant under $\pi/3$ rotations in the basal plane.
[39] G. Asti, in *Ferromagnetic Materials*, edited by K.H.J. Buschow and E.P. Wohlfarth (Elsevier, Amsterdam, 1990), Vol. 5, p. 397.
[40] E.A. Turov and V.G. Shavrov, Zh. Éksp. Teor. Fiz. **43**, 2273 (1962) [Sov. Phys. JETP **16**, 1606 (1963)].
[41] P. Morin *et al.*, J. Magn. Magn. Mater. **81**, 247 (1989).
[42] P. Morin and A. de Combarieu, Solid State Commun. **17**, 975 (1975).
[43] P. Morin *et al.*, Phys. Status Solidi A **24**, 425 (1974).
[44] P. Morin *et al.*, J. Magn. Magn. Mater. **68**, 107 (1987).
[45] M. Amara and P. Morin, Physica B **205**, 379 (1995).
[46] A single-**q** structure is recovered for special values of the phases as, for example, $\phi_2-\phi_1=\pm\pi/2$ and $\phi_3-\phi_1=\pm\pi/2$.
[47] S.A.M. Mentink *et al.*, Phys. Rev. Lett. **73**, 1031 (1994).
[48] C. Lacroix *et al.*, Phys. Rev. Lett. **77**, 5126 (1996).
[49] M.B. Walker *et al.*, J. Phys.: Condens. Matter **6**, 7365 (1994).
[50] K.A. McEwen *et al.*, Physica B **213&214**, 128 (1995).
[51] Y. Baer *et al.*, Solid State Commun. **36**, 387 (1980).
[52] W.J.L. Buyers and T M. Holden, in *Handbook on the Physics and Chemistry of Actinides*, edited by A.J. Freeman and G.H. Lander (North-Holland, Amsterdam, 1985), Vol. 2, p. 239.
[53] K. Andres *et al.*, Solid State Commun. **28**, 405 (1978).
[54] H.R. Ott *et al.*, Physica B **102**, 148 (1980).
[55] U. Steigenberger *et al.*, J. Magn. Magn. Mater. **108**, 163 (1992).
[56] A.I. Goldman *et al.*, Phys. Rev. B **36**, 8523 (1987).